# *PREDICTABILITY OF THE TROPICAL ATMOSPHERE*

J. Shukla

1982

*Tropical Ocean–Atmosphere Newsletter*

**November**

Pages 7–9

TABLE 1 (*Fu and Fletcher*)
*Comparison of variability for $T_s$, $T_w$ and SLO.*

| | Amplitude of seasonal variation | Amplitude of interannual variation for northern summer | Standard deviation for northern summer |
|---|---|---|---|
| $T_s$ (°C) | 23.0 | 10.4 | 2.4 |
| $T_w$ (°C) | 2.0 | 7.6 | 1.8 |
| *SLO* (°C) | | 13.0 | 3.0 |

also show evidence of the approximately 3-year oscillation (Figure 2) found in the tropical Indian and Pacific Oceans (Fu, 1978).

The interannual variability of $T_s$ and $T_w$ are of comparable magnitude (Table 1), but are statistically independent of each other. The correlation coefficients between $T_s$ and *SLO* and between $T_w$ and *SLO* are 0.67 and $-0.73$, indicating that $T_s$ and $T_w$ contribute equally to the interannual variation of *SLO*. The correlation coefficients between $I_M$ and *SLO*, $T_s$ and $T_w$ are 0.61, 0.30 and $-0.52$, respectively, indicating that *SLO* correlates more closely with Indian monsoon rainfall than either $T_s$ or $T_w$.

Table 2 contains a comparison of the thermal conditions on the Tibetan Plateau and in the eastern equatorial Pacific with Indian monsoon rainfall. Of the 9 years with warm Tibetan Plateau, 7 were wet monsoon years and 2 were dry monsoon years. Of the 5 years with cold Tibetan Plateau, 2 were wet monsoon and 3 were dry monsoon. Thus, a warm Tibet/wet monsoon and cold Tibet /dry monsoon occurred 10 of the 14 years. The relationships cold SST/wet monsoon and warm SST/dry monsoon were found 11 of the 14 years.

It is of interest to distinguish between years of strong and weak *SLO*. When the Tibetan Plateau was warm and SST was cold (*i.e.*, a large SLO), a wet monsoon occurred 15 of the 18 years, while for a weak thermal contrast, a dry monsoon occurred only 6 of the 10 years. This suggests that a strong thermal contrast between the heat source and heat sink is a better indicator of Indian monsoon rainfall than a weak thermal contrast.

The conventional notion of the Walker circulation is rising motion over the monsoon region and subsidence over the eastern equatorial Pacific and western Indian Ocean (Newell *et al.*, 1974). Our results suggest that heating over the Tibetan Plateau during northern summer contributes to rising motion over Asia. Because the surface heat budget of the Tibetan Plateau is strongly influenced by the amount and duration of snow cover, it may be possible to predict the Tibetan Plateau temperature anomaly quite independently of Indian rainfall and eastern equatorial SST. These relationships should be useful additions to the growing arsenal of predictors because the season examined is two seasons before the time of the maximum anomalies over North America associated with the southern oscillation anomaly. Further diagnostic studies are needed to explore the possible role of the Tibetan Plateau in "triggering" southern oscillation events. For example, when all necessary conditions are present for a southern oscillation event, a "warm" Tibet could enhance subsidence (and divergence) in the eastern equatorial Pacific, while a "cold" Tibet would have the opposite effect.

TABLE 2 (*Fu and Fletcher*)
*Comparison of the roles of the Tibetan Plateau and SST in the eastern equatorial Pacific in an anomalous Indian monsoon.*

| Region | Thermal condition | Number of total years | Number of wet monsoon years | Number of dry monsoon years |
|---|---|---|---|---|
| Tibetan Plateau | warm | 9 | 7 | 2 |
| | cold | 5 | 2 | 3 |
| 5°N-10°S, 120°W-160°W | warm | 5 | 2 | 3 |
| | cold | 9 | 8 | 1 |

*References*


Banerjee, A. K. and C. R. V. Raman (1976) One hundred years of southwest monsoon rainfall over India. Scientific Report No. 76/6, Meteorological Office, Poona-5.

Bhalme, H. N. and D. A. Mooley (1980) Large-scale drought/floods and monsoon circulation. *Monthly Weather Review, 108*, 1197-1211.

Fu, C. (1978) The effects of tropical ocean on the long term variation of Western Pacific High. *Oceanic Selections*, No. 2, 16-21.

Newell, R. E., J. W. Kidson, D. G. Vincent and G. J. Boer (1974) *The General Circulation of Tropical Atmosphere and Interactions with Extratropical Latitudes, Vol. 2*. The M.I.T. Press, Cambridge, 371 pp.

Yeh, T. C. and Y. X. Gao (1979) *Meteorology on the Tibetan Plateau*. Science Press, Beijing, 278 pp.



Congbin Fu
Joseph O. Fletcher
*Cooperative Institute for Research in Environmental Sciences*
*University of Colorado*
*Boulder, CO 80309*


# Predictability of the Tropical Atmosphere

The theoretical upper limit for deterministic prediction is mainly determined by the growth rate and equilibration of dominant instabilities which exist for a given observed state of the atmosphere. An uncertainty in the initial conditions grows with the characteristic growth rate of the fastest growing instabilities. Nonlinear interactions among different scales of motion help spread this uncertainty to all the scales present in the flow. For a simple hydrodynamical system (barotropic fluid *without β effect* and *without mountain*), Lorenz (1969) showed that different scales of motion have different ranges of predictability and that the theoretical upper limit of predictability ranges from a few days to a few weeks. Several general circulation model studies (Charney *et al.*, 1966; Smagorinsky, 1969) carried out to determine the theoretical upper limit of predictability, have suggested that the doubling time for the error is about three to five days.

Since the error growth rates and their equilibration depend upon the dynamical regime, the magnitude of the error, the initial condition, and the meteorological variable, and since the nature of dymanical instabilities which are most important for day-to-day fluctuations in the tropics are very different from those in the middle latitudes, we have examined the predictability of the tropics and the middle latitudes separately. We present here the summary of the results on predictability of the tropical atmosphere (Shukla, 1981).

We have calculated the error growth rate and predictability of the GLAS (Goddard Laboratory for Atmospheric Sciences) climate model for winter and summer initial conditions. Starting from the initial conditions in the middle of June, the GLAS model was first integrated for 30 days. A second integration for 30 days was also carried out, in which only initial conditions of the east-west ($u$, positive eastward) and north-south ($v$, positive northward) wind fields at all nine levels of the model were randomly perturbed. Each grid point was randomly perturbed corresponding to a Gaussian distribution with zero mean and standard deviation of 3 m $s^{-1}$ for $u$ and $v$ fields. Figure 1 shows the evolution of the initial error for temperature at 500 mb. The solid line, the dashed line and the dotted line refer to the error averaged over a 20° latitude belt centered at 6°N, 30°N and 58°N, respectively. It should be noted that although there was no initial error in the temperature and pressure field, the error in these fields for the first 4-5 days is the largest at 6°N. The same was true for errors in pressure and $u$ and $v$ components. This suggests that the rate of growth of initial error is large in the tropical latitudes compared to

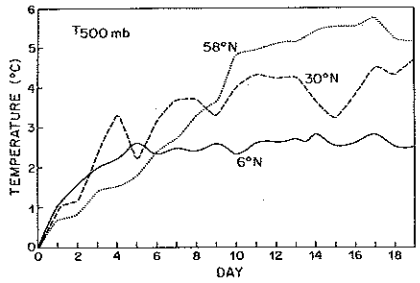


FIGURE 1 (*Shukla*)

*Root mean square as a function of time between a summer control and a predictability run for temperature (°C) at 500 mb. Solid line, dashed line and dotted line refer to an average over 20° latitude belt centered at 6°N, 30°N and 58°N respectively.*

the middle latitudes. The final asymptotic value of the error is the largest for 58°N and the smallest for 6°N. This is due to large day-to-day fluctuations in sea level pressure and temperature in the middle latitudes compared to low latitudes. Due to the smallness of the Coriolis parameter, large changes in pressure and temperature cannot be sustained in the tropics.

Figure 2 shows the zonally averaged ratio of root mean square error and standard deviation of day to day fluctuations for geopotential height for nine pairs of model integrations in which the winter initial conditions of $u$ and $v$ at nine levels of the GLAS climate model were randomly perturbed. It is seen that the ratio is large for the low latitudes compared to the middle latitudes. This indicates that although the error is smaller for the low latitudes, the magnitude of the day-to-day fluctuations is so small that it takes only a few days for the error to be about half of the standard deviation.

These results suggest that the limit of deterministic predictability is much shorter for the tropics (3-7 days) compared to the middle latitudes (10-15 days), due to the following reasons. (a) The growth of initial error is larger because synoptic instabilities in the tropics are driven mainly by condensation and because of the limitations on the physical parameterization of moist convection, incorrect diabatic heat forcing degrades the motion field, which gives even more incorrect heating. (b) Because of the fast growth rate, it takes only a few days for the initial error to become comparable to the maximum error, whose magnitude is very small, as evidenced by low values of standard deviation. These values are low primarily because the amplitudes of the synoptic scale tropical disturbances equilibrate at low values.

The above consideration will apply even for an idealized case of a uniform and high density of observations over the globe. The reality of the situation is, of course, much worse. Tropical areas, even in the northern hemisphere, have far fewer upper air soundings compared to the northern hemispheric middle latitudes; tropical disturbances, being intrinsically of smaller scale, cannot be resolved well; and the error in initial conditions for the tropics is quite high.

The interannual variability of monthly and seasonal means is determined by the combined effects of the internal atmospheric dynamics and the slowly varying 'external' boundary conditions of sea surface temperature (SST), soil moisture, snow/sea ice, *etc.* The tropical circulation is dominated by quasi-stationary heat sources with associated Hadley, Walker and monsoon circulations. Since the space and time scales of these circulations are much larger than those of tropical disturbances (easterly waves, depressions, *etc.*), it is plausible that the time averages in the tropics are potentially more predictable. Fluctuations in the planetary scale tropical circulations (location and intensity of ITCZ, Walker cell, monsoon, *etc.*) are determined primarily by slowly varying boundary forcings. Tropical disturbances are too weak to destabilize the planetary scale circulations. It should be noted with interest that the same factors which cause a lack of short range predictability (as described previously) provide a higher potential for predictability of time averages in the tropics.

Charney and Shukla (1981) have suggested that the time-averaged monsoon circulation is potentially more predictable than the middle latitude circulation because the large-scale monsoon circulation is stable with respect to dynamic instabilities which develop in the monsoon flow, and fluctuations in the boundary conditions have significant effects on the time-averaged monsoon flow.

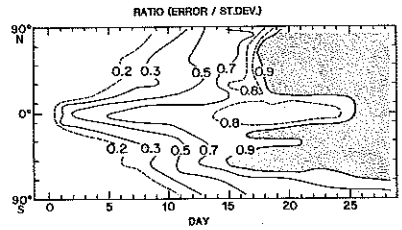


FIGURE 2 (*Shukla*)

*Zonally averaged values of the ratio of root mean square between nine pairs of winter model runs and standard deviation of daily values for geopotential height at 500 mb.*

In this note we have extended the work of Charney and Shukla (1981) by comparing the model variability due to internal dynamics and to changes in the SST boundary condition. One of the limitations of the earlier study was the comparison of the model variability with the observed variability. While this must be the ultimate goal, it is more appropriate first to intercompare two different properties of the same model so that any deficiencies of the model itself do not bias the conclusions.

We carried out a 45-day integration of the GLAS climate model starting from the observed initial conditions in the middle of June and climatological mean boundary conditions of SST. We refer to this integration as control run C. For the identical boundary conditions we carried out three additional integrations for 45 days each by randomly changing the initial conditions of $u$ and $v$ at each of the nine levels of the model. The spatial structure of the random errors corresponded to a Gaussian distribution with zero mean and standard deviation of 3 m $s^{-1}$ for $u$ and $v$ separately. We refer to these three integrations as predictability runs ($P_1$, $P_2$, and $P_3$). Although the statistical properties of the random errors were the same for each predictability run, the actual grid point values were randomly different. We also carried out three additional integrations for which, in addition to the randomly perturbed initial conditions, the boundary conditions of SST between the equator and 30°N were replaced by the observed SST during July of 1972, 1973, 1974. We refer to these three integrations as boundary forcing runs ($B_1$, $B_2$, and $B_3$). Although there were large sytematic differences over a few grid points, the SST anomaly over most of the tropical oceans appeared to be realistic.

The variance $(\sigma_p)^2$ among C, $P_1$, $P_2$, and $P_3$ will give a measure of the natural variability of the model; the variance $(\sigma_B)^2$ among C, $B_1$, $B_2$, and $B_3$ will give a measure of the variability due to changes in the boundary conditions of tropical SST. We also calculated the observed variances $(\sigma_o)^2$ for ten years of observed monthly means.

Figure 3 shows the plots of zonally averaged values of standard deviations $\sigma_p$, $\sigma_B$, $\sigma_o$ and the ratios $\sigma_o/\sigma_p$ and $\sigma_o/\sigma_B$. In agreement with the results of Charney and Shukla (1981), it is seen that the ratio $\sigma_o/\sigma_p$ is more than two in the tropical latitudes and close to one in the middle latitudes. The new result is that the curve $\sigma_B$ lies nearly halfway between the

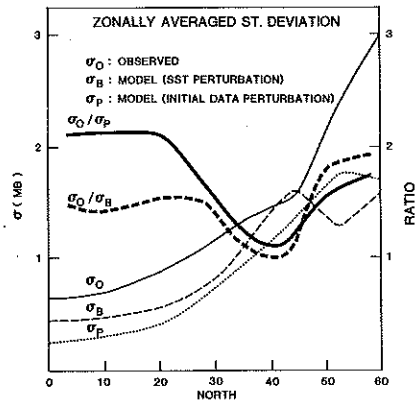


FIGURE 3 (*Shukla*)

*Zonally averaged standard deviation among monthly mean (July) sea level pressure (mb) for 10 years of obervations ($\sigma_o$, thin solid line); four model runs with variable boundary conditions ($\sigma_B$, thin dashed line); and four model runs with identical boundary conditions ($\sigma_p$, thin dotted line). Thick solid line and thick dashed line show the ratio $\sigma_o/\sigma_p$ and $\sigma_o/\sigma_B$ respectively.*

curves $\sigma_o$ and $\sigma_p$. This suggests that about half of the remaining variability for this model is accounted for by changes in SST between the equator and 30°N.

These conclusions are further supported by a more comprehensive study by Manabe and Hahn (1981) who integrated the GFDL (Geophysical Fluid Dynamics Laboratory) spectral climate model for 15 years with prescribed but seasonally varying boundary condition of SST. They found that the ratio of zonally averaged values of standard deviation of seasonal mean for observations and model simulations was about two in the near equatorial regions and reduced to about one in the middle and high latitudes.

This supports our earlier hypothesis that the slowly varying boundary conditions play an important role in determining the interannual variability of time averages for the tropics. Additional effects of soil moisture (Shukla and Mintz, 1982) or snow cover could possibly bring the $\sigma_o$ and $\sigma_B$ curves still closer. It is however to be noted that the long period internal dynamical changes (tropical-extratropical interactions, *etc.*) also contribute to the interannual variability of time averages, and boundary forcings alone cannot explain the total observed variance.

It is reasonable to conclude that although for short and medium range the instantaneous state of the tropical atmosphere is less predictable, the time averages (monthly and seasonal means) are potentially more predictable in the tropics. Since there is sufficient observational, theoretical and numerical model experimental evidence that tropical heat sources can also influence the middle latitude circulation, it is likely that the monthly means for middle latitudes could also be potentially predictable due to their interaction with low latitudes.

*References*


Charney, J. G., R. G. Fleagle, V. E. Lally, H. Riehl and D. Q. Wark (1966) The feasibility of a global observation and analysis experiment. *Bulletin of the American Meteorological Society, 47,* 200-220.

Charney, J. G. and J. Shukla (1981) Predictability of monsoon. In: *Monsoon Dynamics,* J. Lighthill and R. P. Pearce, editors, Cambridge University Press, Cambridge, 99-109.

Lorenz, E. N. (1969) The predictability of a flow which possesses many scales of motion. *Tellus, 21,* 289-306.

Manabe, S. and D. G. Hahn (1981) Simulation of atmospheric variability. *Monthly Weather Review, 109,* 2260-2286.

Shukla, J. (1981) Predictability of the tropical atmosphere. NASA Technical Memorandum 83829, Laboratory for Atmospheric Sciences, NASA Goddard Space Flight Center, Greenbelt, MD, 51 pp.

Shukla, J. and Y. Mintz (1981) The influence of land-surface evapotranspiration on the earth's climate. *Science, 215,* 1498-1501.

Smagorinsky, J. (1969) Problems and promises of deterministic extended range forecasting. *Bulletin of the American Meteorological Society, 50,* 286-311.



Jagadish Shukla
*Laboratory for Atmospheric Sciences*
*NASA/Goddard Space Flight Center*
*Greenbelt, MD 20771*


# Erosion of Potential Vorticity Gradients by Critical Layers in the Atlantic North Equatorial Current

Bretherton (1966) showed that the presence of a critical layer, which occurs at depth $z_c$ when $\bar{U}(z_c) = c_p$, where $\bar{U}(z)$ is the zonal mean flow profile and $c_p$ is a disturbance phase speed, implies the instability of the flow. At depth $z_c$ the particle speed equals the phase speed and a given particle is always exposed to the same phase of a wave cycle. Particles which are initially moving north will continue to do so, and conversely, southward moving particles continue to move south. These excursions imply a large north-south flux of potential vorticity *unless* the potential vorticity gradient ($Q_y$) vanishes at $z_c$. If $Q_y \neq 0$, the resulting flux of potential vorticity can only be balanced by growth of the instability.

Using the POLYMODE Array III Cluster C data set, Keffer (1982a) found four independent pieces of evidence for the existence of a critical layer at 300 m depth within the Atlantic North Equatorial Current. (1) The 3.5 cm $s^{-1}$ westward cross-correlation phase velocity corresponds to the 300 m flow velocity. (2) The primary temperature balance at 300 m is $T'_t + \bar{U}T'_x = 0$, where $T'$ is the temperature perturbation measured at the current meters. (3) The moored temperature measurements indicated a maximum eddy potential energy at 300 m. (4) Historical Nansen bottle data from the National Oceanographic Data Center (NODC) indicated a maximum eddy potential energy at 300 m.

Given the existence of a critical layer and the importance of the north-south eddy flux of potential vorticity, it becomes important to ask: What is the mean potential vorticity gradient at $z_c$?

Figure 1 is a contour plot of potential vorticity along the GEOSECS cruise track (~50°W) in the western Atlantic from McDowell *et al.* (1982). Potential vorticity was evaluated from

$$Q = -\frac{f}{\rho}\frac{\partial \rho_\theta}{\partial z}$$

where $\partial\rho_\theta/\partial z$ is the vertical adiabatic density gradient, $\rho$ is the density and $f$ is the Coriolis parameter. In Figure 1, $Q$ is contoured as a function of surface referenced density anomaly ($\sigma_\theta$) and latitude. Such a prescription for $Q$ is consistent for large scale slow motions where relative vorticity and horizontal components of vorticity are small.

Also shown in the North Equatorial Current area is a curve representing the density at

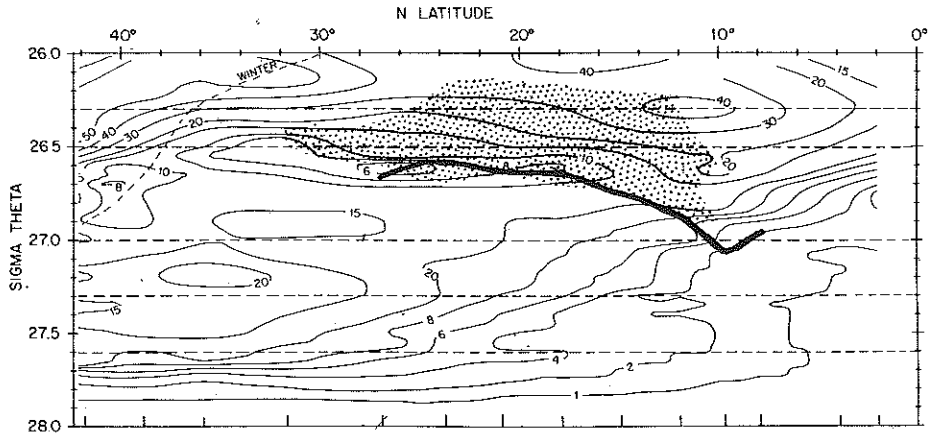


FIGURE 1 *(Keffer)*

*Potential vorticity ($10^{-13}$ $cm^{-1}$ $s^{-1}$) along 50°W computed from GEOSECS data and contoured as a function of density ($\sigma_\theta$) and latitude. The stippled region is where $Q_y < 0$ and these latitudes will be a likely site of baroclinic instability. Just below this region is a heavy solid line that marks the 300 m isodepth. Note that at 15°N, $Q_y \rightarrow 0$ at this depth. This may be due to critical layer homogenization. The dashed line is the winter outcrop.*

300 m. Recall that it was at this depth, at the Cluster C site (15°N), that a critical layer was observed. Remarkably, $Q_y \rightarrow 0$ at the Cluster C latitude. Indeed, close examination of the $Q_y(z)$ profile (Figure 2) used in Keffer (1982a) to calculate shear modes, shows that the sign reversal happens at 300 m. This comes from a completely independent data set using NODC Nansen bottle data.

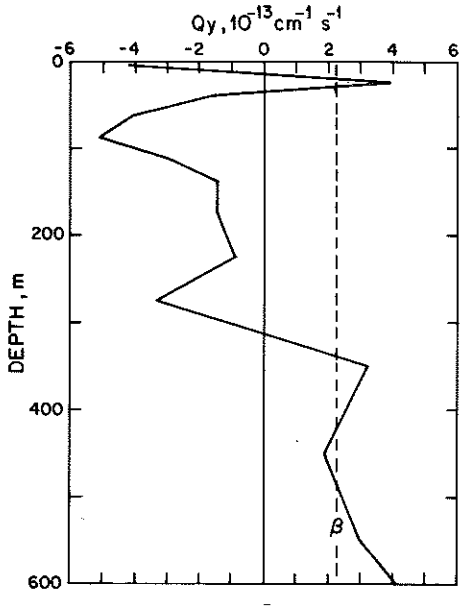


FIGURE 2 *(Keffer)*
*Northward potential vorticity gradient ($Q_y$) calculated as $Q_y = \beta - (f\bar{\rho}_y/\bar{\rho}_z)_z$ from historical data (Keffer, 1982b). The dashed line is the planetary vorticity gradient* β. *Note that $Q_y \rightarrow 0$ at 300 m.*

Pedlosky (1982) described a two-layer model in which a critical layer and a weak potential vorticity gradient are present in the lower layer. The mean shear is slightly supercritical. In the limit of low frequency, slightly dissipative waves, an instability develops, grows, and then feeds back to the mean flow and potential vorticity gradients, resulting in a finite-amplitude state where the potential vorticity gradient in the lower layer (*i.e.*, the critical layer) has been homogenized. Although this is a simple model, more physical arguments, such as Bretherton's (1966), would also suggest that potential vorticity gradients within a critical layer may be especially susceptible to erosion and eventual homogenization due to the large particle excursions in the layer.

Cluster C is located far downstream in a 2500 km long current, and most likely will be observing the finite-amplitude state of any developing waves and resulting potential vorticity gradient. Indeed, no significant downgradient heat fluxes were observed (Keffer, 1982b).

Two additional questions suggest themselves. First, from Figure 1, it can be seen that the isopycnal $\sigma_\theta = 26.8$ that is suspected of containing a critical layer at the Cluster C laititude and where $Q_y \rightarrow 0$, is the same isopycnal that has undergone extensive homogenization within the subtropical gyre (latitudes 20°-36°) due to processes described by Rhines and Young (1982). This may be coincidence or it may be due to the interactions between the two processes.

Second, although the condition $Q_y \rightarrow 0$ at $z_c$ removes the requirement for critical layer instability, it is unclear what it implies for baroclinic instability in general.

*References*


Bretherton, F. P. (1966) Critical layer instability in baroclinic flows. *Quarterly Journal of the Royal Meteorological Society, 92,* 325-334.

Keffer, T. (1982a) Time dependent temperature and vorticity balances in the Atlantic North Equatorial Current. *Journal of Physical Oceanography,* in press.

Keffer, T. (1982b) The baroclinic stability of the Atlantic North Equatorial Current. *Journal of Physical Oceanography,* submitted.

McDowell, S. E., P. B. Rhines and T. Keffer (1982) Maps of potential vorticity in the North Atlantic and their relation to the general circulation. *Journal of Physical Oceanography,* in press.

Pedlosky, J. (1982) A simple model for nonlinear critical layers in an unstable baroclinic wave. *Journal of Fluid Mechanics,* in press.

Rhines, P. B. and W. R. Young (1982) Homogenization of potential vorticity in planetary gyres. *Journal of Fluid Mechanics,* in press.



Tom Keffer
*Department of Physical Oceanography*
*Woods Hole Oceanographic Institution*
*Woods Hole, MA 02543*


# The 1978 Occurrence of High Sea Surface Salinity in the Eastern Coral Sea

Long-term changes in sea surface salinity in the Coral Sea, including high salinity values occurring in the periods 1957-58 and 1972-73, have been described by Donguy and Henin (1975). These phenomena were related to the El Niño events along the western coast of South America (Donguy and Henin, 1981). During these periods the Intertropical Convergence Zone (ITCZ) was on the equator and the eastward flowing South Equatorial Countercurrent (SECC) was particularly noticeable north of 10°S. South of this latitude a strong westward current advected high salinity waters. At the same time, drastic drought conditions occurred in southwest Pacific countries.

During 1978, when high sea surface salinities were observed (Figure1) in the eastern Coral Sea, the El Niño phenomenon did not occur in the eastern Pacific Ocean. In this note an attempt is made to determine whether changes in the current system explain the salinity variation. Generally, in the southwest Pacific Ocean, eastward flows carry low salinity water and westward flows transport saltier water.

The mean height of the surface dynamic topography relative to 1000 decibars is quite variable in the Coral Sea. A zonal ridge is commonly observed near 15-18°S, inducing an eastward flow on the south side (the South

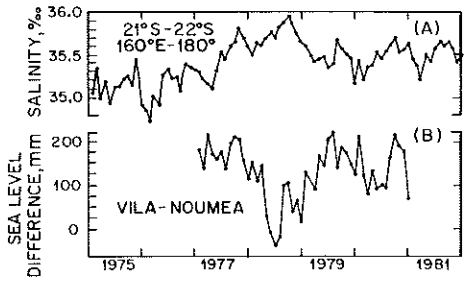


FIGURE 1 *(Henin)*
*(A) Monthly mean sea surface salinities recorded 1975-81 by merchant ships between 21°S-22°S and 160°E-180°. (B) Monthly mean sea level differences between Vila (17°26.4'S, 168°11.4'E) and Noumea (22°10.8'S, 166°15.6'E) during 1977 to 1981.*

Tropical Countercurrent, STCC), a westward flow on the north side (the South Equatorial Current, SEC) and the eastward flowing South Equatorial Countercurrent (SECC) which passes through the Solomon Archipelago.

Scarcity of hydrological casts in the Coral Sea prompted the development of data collection using XBT measurements from merchant ships. In this way, data have been collected routinely along shipping lanes between New Caledonia and Japan, New Guinea, Vanuatu and Fiji (Meyers and Donguy, 1980). However, the XBT program only became operational in 1979, so no data are available to infer the current system during 1978 when the high salinities were observed.

The relationship between monthly mean values of dynamic height and sea level in tropical areas (Wyrtki, 1980) was exploited to monitor the current system variations in the Coral Sea. Sea level data from three stations were used. Honiara (Solomon Islands) lies in the dynamic trough between the SECC and the